Physics – Uspekhi **49** (10) 1003 – 1016 (2006)

REVIEWS OF TOPICAL PROBLEMS PACS numbers: 74.20.De, **74.25.–q**, 74.70.Ad

Ginzburg – Landau theory: the case of two-band superconductors

I N Askerzade

DOI: 10.1070/PU2006v049n10ABEH006055

Contents

Abstract. Recent studies of two-band superconductors using the Ginzburg – Landau (GL) theory are reviewed. The upper and lower critical fields [$H_{c2}(T)$ and $H_{c1}(T)$, respectively], thermodynamic magnetic field $H_{cm}(T)$, critical current density $j_c(T)$, magnetization $M(T)$ near the upper critical field, and the upper critical field $H_{c2}^{film}(T)$ of thin films are examined from the viewpoint of their temperature dependence at a point T_c using the two-band GL theory. The results are shown to be in good agreement with the experimental data for the bulky samples of superconducting magnesium diboride, MgB_2, and nonmagnetic borocarbides $LuNi_2B_2C$ and YNi_2B_2C. The specific heat jump turns out to be smaller than that calculated by single-band GL theory. The upper critical field of thin films of two-band superconductors is calculated and the Little – Parks effect is analyzed. It is shown that magnetic flux quantization and the relationship between the surface critical magnetic field $H_{c3}(T)$ and the upper critical field $H_{c2}(T)$ are the same as in the single-band GL theory. Extension of the two-band GL theory to the case of layered anisotropy is presented. The anisotropy parameter of the upper critical field H_{c2} and the London penetration depth λ, calculated for MgB_2 single crystals, are in good agreement with the experimental data and show opposite temperature behavior to that in single-band GL theory.

I N Askerzade Institute of Physics, Azerbaijan National Academy of Sciences, H Cavid prosp. 33, Az1143 Baku, Azerbaijan
Tel. (99412) 439 34 16. Fax (99412) 439 59 61
E-mail: solstphs@physics.ab.az
Department of Physics, Faculty of Sciences, Ankara University, 06100, Tandogan, Ankara, Turkey
E-mail: iasker@science.ankara.edu.tr

Received 25 January 2006
Uspekhi Fizicheskikh Nauk **176** (10) 1025 – 1038 (2006)
Translated by I N Askerzade; edited by A Radzig

1. Introduction

The discovery of superconductivity in MgB_2 [1] has attracted considerable attention. MgB_2 compound holds the highest superconducting transition temperature, about $T_c = 40$ K, among binary compounds of a relatively simple crystal structure. Additionally, MgB_2 has a high potential to replace conventional superconducting materials in electronics applications. Large critical densities have already been reported for bulky samples [2] and bulk superconductivity was established immediately to support supercurrent transport between granules [3]. The material shows a pronounced isotope effect [4]. Measurements of the nuclear spin – lattice relaxation rate [5] indicate that MgB_2 constitutes a Bardeen – Cooper – Schrieffer (BCS) type superconductor with phonon-mediated pairing. Calculations of the band structure and the phonon spectrum predict a double energy gap [6, 7], with a larger gap being attributed to two-dimensional p_{x-y} orbitals, and a smaller gap attributed to three-dimensional p_z bonding and anti-bonding orbitals. A two-band character of the superconducting state in MgB_2 is clearly evident in recently performed tunnel measurements [8, 9] and specific heat measurements [10].

The other class of superconductors (SCs) comprises rare-earth transition-metal borocarbides with the general formula RNi_2B_2C, which have attracted the interest of many researchers because of their wide variety of physical properties: compounds with $R =$ Lu, Y exhibit fairly high superconducting transition temperatures T_c of about 15 – 16 K [11]; magnetism coexists with superconductivity for $R =$ Dy, Ho, Er, and Tm [12], whereas only antiferromagnetic order occurs for $R =$ Pr, Nd, Sm, Gd, and Tb [13]. These compounds show a layered structure and therefore they are considered as possibly close to quasi-2D cuprates. However, various band structure calculations within the local density approximation

[14 – 17] clearly indicated the 3D electronic structure. Quantum oscillation measurements in nonmagnetic borocarbides $LuNi_2B_2C$ and YNi_2B_2C give clear evidence of a multiband character in the normal state [18].

The magnetic phase diagram for MgB_2, $LuNi_2B_2C$, and YNi_2B_2C compounds has also been of interest to researchers. In contrast to conventional superconductors, the upper critical field for a bulky MgB_2, $LuNi_2B_2C$, and YNi_2B_2C has a positive curvature near T_c [19 – 22]. To understand the nature of the unusual behavior at a microscopic level, a two-band (TB) Eliashberg model of superconductivity was first proposed by Shulga et al. [23] for $LuNi_2B_2C$ and YNi_2B_2C, and recently for MgB_2 [24]. Here, it is necessary to remark that the generalization of the BCS theory to the multiband model was first suggested in Refs [25, 26] many years ago. The recent development of the two-band BCS theory, taking into account van Hove singularity of the density of states, was presented in Ref. [27].

The temperature dependence of the thermodynamic critical magnetic field $H_{cm}(T)$ remains to be determined theoretically. The temperature dependence of $H_{cm}(T)$ is essential for the assessment of the behavior of specific heat at temperatures close to T_c. It is generally known that BCS calculations, which implicitly incorporate an isotropic single-band Fermi surface, reveal that the jump in specific heat at T_c is constant at a magnitude of 1.43. The Eliashberg theory, assuming a strong electron – phonon coupling, would be expected to give a value greater than 1.43. Several groups have measured specific heat of magnesium diboride, MgB_2 [10, 28]. The measured specific heat shows a small jump at T_c, which is not explained within the standard BCS and Eliashberg theories. The *ab initio* calculations of specific heat in two-band Eliashberg theory were done by Golubov et al. [29].

Although extensive theoretical studies at the microscopic level were carried out after the discovery of borocarbides and magnesium diboride, it is necessary to gather additional information about its superconducting properties by using the macroscopic Ginzburg – Landau theory [30]. Regardless of the origin of superconductivity, the GL theory has been found to be adequate for explaining the measurable macroscopic quantities. The temperature dependences of fundamental measurable quantities like the lower critical field H_{c1} and the upper critical field H_{c2} are expected to help in understanding the mechanism of superconductivity. The $H_{c2}(T)$ and $H_{c1}(T)$ temperature dependences in borocarbides are different from those of the single-band (SB) s-wave BCS theory and GL theory. The different temperature dependences may indicate a slight difference in the pairing state of the superconductor.

In this review paper, we summarize recent studies using the two-band GL theory and apply it to determining the temperature dependence of $H_{c2}(T)$, $H_{c1}(T)$, and $H_{cm}(T)$ for nonmagnetic borocarbides and magnesium diboride. We will show that the presence of two order parameters in the theory leads to a nonlinear temperature dependence which is shown to be in good agreement with experimental data for two-band MgB_2, $LuNi_2B_2C$, and YNi_2B_2C superconductors. Quantization of the magnetic flux, Little – Parks oscillations of critical temperature, and the relationship between the surface critical field $H_{c3}(T)$ and upper critical field $H_{c2}(T)$ in the framework of the two-band GL theory will also be considered. The layout of the paper is as follows. In Section 2 we will derive the two-band GL equations for isotropic superconductors and these equations will be applied to the calculations of several physical quantities. At the end of this section, a generalization of the TB GL theory to the case of layered anisotropy is considered. The anisotropy parameters of the upper critical field H_{c2} and London penetration depth λ were calculated within this approach. Section 3 is devoted to the results obtained and their discussion. In Section 4 conclusions will be drawn.

2. Theory

In the presence of two order parameters (OPs) in an isotropic s-wave superconductor, the Ginzburg – Landau functional of free energy can be written down as [31 – 33]

$$F[\Psi_1, \Psi_2] = \int d^3r \left(F_1 + F_{12} + F_2 + \frac{H^2}{8\pi} \right), \tag{1}$$

with

$$F_i = \frac{\hbar^2}{4m_i} \left| \left(\nabla - \frac{2\pi i \mathbf{A}}{\Phi_0} \right) \Psi_i \right|^2 + \alpha_i(T) \Psi_i^2 + \frac{\beta_i}{2} \Psi_i^4 , \tag{2}$$

$$F_{12} = \varepsilon(\Psi_1 \Psi_2^* + \text{c.c.}) + \varepsilon_1 \left[\left(\nabla + \frac{2\pi i \mathbf{A}}{\Phi_0} \right) \Psi_1^* \left(\nabla - \frac{2\pi i \mathbf{A}}{\Phi_0} \right) \Psi_2 + \text{c.c.} \right] . \tag{3}$$

Here, m_i denotes the effective mass of the carriers belonging to the i band ($i = 1, 2$); F_i is the free energy of separate bands; the coefficient α is given by $\alpha_i = \gamma_i(T - T_{ci})$, which depends on temperature linearly, γ_i is the proportionality constant, while the coefficient β_i is independent of temperature; $\mathbf{H}$ is the external magnetic field, and $\mathbf{H} = \text{rot}\,\mathbf{A}$. The quantities ε and ε_1 describe interband mixing of two order parameters and their gradients, respectively.

Minimization of the free energy functional with respect to the order parameters yields GL equations for two-band superconductors in one-dimensional case for $\mathbf{A} = (0, Hx, 0)$:

$$-\frac{\hbar^2}{4m_1} \left(\frac{d^2}{dx^2} - \frac{x^2}{l_s^4} \right) \Psi_1 + \alpha_1(T) \Psi_1 + \varepsilon \Psi_2 + \varepsilon_1 \left(\frac{d^2}{dx^2} - \frac{x^2}{l_s^4} \right) \Psi_2 + \beta_1 \Psi_1^3 = 0 , \tag{4a}$$

$$-\frac{\hbar^2}{4m_2} \left(\frac{d^2}{dx^2} - \frac{x^2}{l_s^4} \right) \Psi_2 + \alpha_2(T) \Psi_2 + \varepsilon \Psi_1 + \varepsilon_1 \left(\frac{d^2}{dx^2} - \frac{x^2}{l_s^4} \right) \Psi_1 + \beta_2 \Psi_2^3 = 0 , \tag{4b}$$

where $l_s^2 = \hbar c/(2eH)$ is the so-called magnetic length. In deriving the last equations without losing generality, we consider for simplicity the case in which Ψ and $\mathbf{A}$ depend only on a single coordinate x. Boundary conditions for two-band GL equations have the form

$$\mathbf{n} \left(\nabla - \frac{2\pi i \mathbf{A}}{\Phi_0} \right) \Psi_1 = a \Psi_1 + b \Psi_2 , \tag{5a}$$

$$\mathbf{n} \left(\nabla - \frac{2\pi i \mathbf{A}}{\Phi_0} \right) \Psi_2 = c \Psi_1 + d \Psi_2 , \tag{5b}$$

where a, b, c, and d are constants, and $\mathbf{n}$ is a unit vector normal to the superconductor surface. Here, it necessary to remark that two-band Ginzburg – Landau equations were first discussed by Moskalenko [34]. However, terms describing intergradient interaction were absent in equations presented in Ref. [34], unlike those entering equations (4a) and (4b). In paper [34], the upper critical field problem was only discussed in the linear approximation. As will be shown in Sections 3.1, 3.3, and 3.11, inclusion of the term with intergradient interaction in the equations leads to interesting results.

Considering $\Psi_i(\mathbf{r}) = |\Psi_i(\mathbf{r})| \exp(\mathrm{i}\phi_i(\mathbf{r}))$ in Eqns (1)–(3), with $\phi_i(\mathbf{r})$ being the phase of the OP, and $|\Psi_i(\mathbf{r})|$ the modulus of the OP, we can obtain the equilibrium values for $|\Psi_i(\mathbf{r})|$ in the absence of any external magnetic fields:

$$|\Psi_{10}|^2 = -\frac{\alpha_2^2(T)\big(\alpha_1(T)\,\alpha_2(T) - \varepsilon^2\big)}{\varepsilon^2\beta_2\alpha_1(T) + \beta_1\alpha_2^3(T)}\,, \tag{6a}$$

$$|\Psi_{20}|^2 = -\frac{\alpha_1^2(T)\big(\alpha_1(T)\,\alpha_2(T) - \varepsilon^2\big)}{\varepsilon^2\beta_1\alpha_2(T) + \beta_2\alpha_1^3(T)}\,. \tag{6b}$$

The OP phase difference at equilibrium can be given as

$$\cos(\phi_1 - \phi_2) = 1 \qquad \text{if} \quad \varepsilon < 0\,, \tag{7a}$$

$$\cos(\phi_1 - \phi_2) = -1 \qquad \text{if} \quad \varepsilon > 0\,. \tag{7b}$$

2.1 Upper critical field $H_{c2}(T)$

It is well known that $H_{c2}(T)$ for the single-band SC can be calculated as the lower eigenvalue problem of the linearized GL equation [35]. In the vicinity of T_c we can neglect cubic terms in Eqns (4a), (4b). Then Eqns (4a) and (4b) can be rewritten as

$$-\frac{\hbar^2}{4m_1}\left(\frac{\mathrm{d}^2}{\mathrm{d}x^2} - \frac{x^2}{l_s^4}\right)\Psi_1 + \alpha_1(T)\Psi_1 + \varepsilon\Psi_2 + \varepsilon_1\left(\frac{\mathrm{d}^2}{\mathrm{d}x^2} - \frac{x^2}{l_s^4}\right)\Psi_2 = 0\,, \tag{8a}$$

$$-\frac{\hbar^2}{4m_2}\left(\frac{\mathrm{d}^2}{\mathrm{d}x^2} - \frac{x^2}{l_s^4}\right)\Psi_2 + \alpha_2(T)\Psi_2 + \varepsilon\Psi_1 + \varepsilon_1\left(\frac{\mathrm{d}^2}{\mathrm{d}x^2} - \frac{x^2}{l_s^4}\right)\Psi_1 = 0\,. \tag{8b}$$

One can arrive at identical equations for $\Psi_1(x)$ and $\Psi_2(x)$ by elimination of unknowns from equations (8). Therefore, we can suppose that $\Psi_1(x) = C\Psi_2(x)$. The coefficient C is obtained by solving the set of equations (8a) and (8b). Substituting the eigenfunction $\Psi_1(x) \propto \exp(-\delta x^2/2)$ corresponding to a lower energy state and taking into account the relationship $\Psi_1(x) = C\Psi_2(x)$, we then obtain expressions for the coefficient C:

$$C = -\frac{\varepsilon - \varepsilon_1\delta}{\big[\hbar^2/(4m_1)\big]\delta + \alpha_1}\,, \qquad C = -\frac{\big[\hbar^2/(4m_2)\big]\delta + \alpha_2}{\varepsilon - \varepsilon_1\delta}\,, \tag{9}$$

which are equivalent to the following equation

$$\left(\frac{\hbar^2}{4m_1}\,\delta + \alpha_1\right)\left(\frac{\hbar^2}{4m_2}\,\delta + \alpha_2\right) = (\varepsilon - \varepsilon_1\delta)^2\,. \tag{9$'$}$$

Using Eqn (9′) one finds the normalized upper critical field of a two-band SC in the isotropic case $h_{c2} = H_{c2}(T)/\tilde{H}_{c2}(0)$, $\tilde{H}_{c2}(0) = cT_c(\gamma_1 m_1 + \gamma_2 m_2)/(\hbar e)$:

$$h_{c2}(\theta) = a_0^{-1}\big(-\theta - c_0 + (A\theta^2 + B\theta + c_0^2)^{1/2}\big)\,, \qquad \theta = \frac{T}{T_c} - 1\,, \tag{10}$$

where the following notation is applied:

$$A = \frac{(x-1)^2}{(x+1)^2} + A_1\eta^2\,, \qquad A_1 = 64\,\frac{a_1 a_2 x^2}{(x+1)^2}\,, \qquad x = \frac{\gamma_1 m_1}{\gamma_2 m_2}\,, \qquad \eta = \frac{T_c m_2 \varepsilon_1 \gamma_2}{\hbar^2\varepsilon}\,, \tag{10a}$$

$$B = \frac{2(x-1)(a_1 x - a_2)}{(x+1)^2} + (a_1 + a_2)A_1\eta^2 + 2B_1\eta\,, \qquad a_i = 1 - \frac{T_{ci}}{T_c}\,, \tag{10b}$$

$$c_0 = \frac{a_1 x + a_2}{x+1} + B_1\eta\,, \qquad a_0 = 1 - \frac{16x\eta^2\varepsilon^2}{\gamma_1\gamma_2 T_c^2}\,. \tag{10c}$$

The critical temperature of a two-band SC is determined from Eqn (9′) in the absence of an external magnetic field:

$$(T_c - T_{c1})(T_c - T_{c2}) = \frac{\varepsilon^2}{\gamma_1\gamma_2}\,. \tag{11}$$

Near T_c, we have asymptotic behavior of h_{c2} in the form

$$h_{c2}(\theta) = a_0^{-1}\left[-\left(1 - \frac{B}{2c_0}\right)\theta + \frac{A}{2c_0}\,\theta^2\right]. \tag{12}$$

2.2 Surface magnetic field $H_{c3}(T)$

In the case of single-band superconductivity, the surface critical field is determined from the GL equation with the vector-potential in the form of $A = H(x - x_0)$ [36]. Such a procedure allows one to obtain an exact value of $H_{c3}(T)$ but requires rather sophisticated numerical calculations. However, a simple variational analysis provides us with an almost exact solution [37]. The accuracy of simple variational procedure is about 2% and can be improved by choosing a proper trial function [38]. As a result, the problem of solving GL equations may be presented as a variational problem of finding the minimum of the free energy functional for the single-band SC [37, 38].

For the trial solutions we substitute functions $\Psi_1(x) \propto \exp(-\delta x^2/2)$ and $\Psi_1(x) = C\Psi_2(x)$ into Eqn (8a) with appropriate boundary conditions

$$\Psi_1(x \to \infty) = 0\,, \qquad \frac{\mathrm{d}\Psi_1}{\mathrm{d}x}(0) = 0\,. \tag{13}$$

The coefficient δ must be determined from the minimum condition for the free energy functional (1). Taking into account the expression for the vector-potential $A = H(x - x_0)$ and using the above-introduced trial functions, we can rewrite expression (1) as follows (here we neglected

quartic terms):

$$\Delta F = \int_0^\infty \mathrm{d}x \left\{ \frac{\hbar^2}{4m_1} \left[\frac{\mathrm{d}^2}{\mathrm{d}x^2} + \left(\frac{2\pi H(x-x_0)}{\Phi_0} \right)^2 + \alpha_1(T) \right] + \frac{1}{C^2} \frac{\hbar^2}{4m_2} \left[\frac{\mathrm{d}^2}{\mathrm{d}x^2} + \left(\frac{2\pi H(x-x_0)}{\Phi_0} \right)^2 + \alpha_2(T) \right] + \frac{2\varepsilon}{C} + \frac{2\varepsilon_1}{C^2} \left(\frac{2\pi H(x-x_0)}{\Phi_0} \right)^2 \right\} \exp\left(-\delta x^2\right). \tag{14}$$

After integration we will first find the minimum of the free energy (14) with respect to x_0. Differentiation with respect to x_0 gives

$$x_0 = (\pi\delta)^{-1/2}. \tag{15}$$

Next, we will find the minimum of the energy functional (14) with respect to δ. This leads to a relationship between δ and C in the following form

$$C^2 \frac{\hbar^2}{4m_1} \left(\alpha_1(T) + \delta\right) + 2C(\varepsilon - \varepsilon_1\delta) + \frac{\hbar^2}{4m_2} \left(\alpha_2(T) + \delta\right) = 0, \tag{16}$$

which is equivalent to Eqn (9′). By substituting Eqns (15) and (16) into Eqn (14) with $\Delta F = 0$, we can then obtain a formula for the surface critical field H_{c3}:

$$\left(\frac{2\pi H}{\Phi_0} \right)^2 \left(1 - \frac{2}{\pi} \right) = \delta^2, \tag{17}$$

where δ is determined from equation (9′), which is consistent with the result found in Ref. [32].

Finally, the surface critical field can be given as

$$H_{c3}(T) = \left(\frac{\pi}{\pi - 2} \right)^{1/2} \frac{\Phi_0 \delta}{2\pi} = 1.66 H_{c2}(T), \tag{18}$$

where $H_{c2}(T)$ is determined by Eqn (10).

2.3 Lower critical field $H_{c1}(T)$

For temperatures near T_c and magnetic fields slightly stronger than H_{c1}, the influence of the field on the moduli of the order parameters Ψ_1 and Ψ_2 can be neglected and therefore we assume $|\Psi_1| = \text{const}$, $|\Psi_2| = \text{const}$. Then, the wave function can be written down as $\Psi_i(\mathbf{r}) = |\Psi_i(\mathbf{r})| \exp\left(\mathrm{i}\phi_i(\mathbf{r})\right)$. Here, $\phi_i(\mathbf{r})$ are the phases of the order parameters, and the GL free energy functional (1) can be rewritten as

$$F[\phi_1, \phi_2] = \int \mathrm{d}^3 r \left[\frac{\hbar^2}{8m_1} n_1(T) \left(\frac{\mathrm{d}\phi_1}{\mathrm{d}\mathbf{r}} - \frac{2\pi \mathbf{A}}{\Phi_0} \right)^2 + \frac{\hbar^2}{8m_2} n_2(T) \left(\frac{\mathrm{d}\phi_2}{\mathrm{d}\mathbf{r}} - \frac{2\pi \mathbf{A}}{\Phi_0} \right)^2 + \varepsilon \left(n_1(T)\, n_2(T) \right)^{1/2} \times \cos(\phi_1 - \phi_2) + \varepsilon_1 \left(n_1(T)\, n_2(T) \right)^{1/2} \cos(\phi_1 - \phi_2) \times \left(\frac{\mathrm{d}\phi_1}{\mathrm{d}\mathbf{r}} - \frac{2\pi \mathbf{A}}{\Phi_0} \right) \left(\frac{\mathrm{d}\phi_2}{\mathrm{d}\mathbf{r}} - \frac{2\pi \mathbf{A}}{\Phi_0} \right) + \frac{H^2}{8\pi} \right], \tag{19}$$

where $n_1(T) = 2|\Psi_1|^2$ and $n_2(T) = 2|\Psi_2|^2$ are the densities of superconducting electrons for the corresponding bands. The temperature dependences $n_1(T)$, $n_2(T)$, and $\phi_1 - \phi_2$ are defined by the equilibrium values of order parameters $|\Psi_1|$ and $|\Psi_2|$, which satisfy the two-band GL equations without linearization [see Eqns (6a), (6b)]. The equations determining the equilibrium values of magnetic field and the OP phases would be obtained by minimizing the free energy functional (19) with respect to the vector-potential $\mathbf{A}$ and the phases ϕ_1, ϕ_2. The equation for the vector-potential takes the form

$$\frac{\nabla \times \nabla \times \mathbf{A}}{4\pi} = \frac{2\pi}{\Phi_0} \left\{ \frac{\hbar^2}{4m_1} n_1(T) \left(\frac{\mathrm{d}\phi_1}{\mathrm{d}\mathbf{r}} - \frac{2\pi \mathbf{A}}{\Phi_0} \right) + \frac{\hbar^2}{4m_2} n_2(T) \left(\frac{\mathrm{d}\phi_2}{\mathrm{d}\mathbf{r}} - \frac{2\pi \mathbf{A}}{\Phi_0} \right) + \varepsilon_1 \left(n_1(T)\, n_2(T) \right)^{1/2} \times \cos(\phi_1 - \phi_2) \left[\left(\frac{\mathrm{d}\phi_1}{\mathrm{d}\mathbf{r}} - \frac{2\pi \mathbf{A}}{\Phi_0} \right) + \left(\frac{\mathrm{d}\phi_2}{\mathrm{d}\mathbf{r}} - \frac{2\pi \mathbf{A}}{\Phi_0} \right) \right] \right\}. \tag{20}$$

By using the appropriate Maxwell equation $\nabla \times \mathbf{H} = (4\pi/c)\mathbf{J}$ (for the magnetostatic case), Eqn (20) leads to the London equation [when taking into account the equilibrium value of the phase differences (7a), (7b)] in the form

$$\lambda^2 \frac{\mathrm{d}^2 H}{\mathrm{d}r^2} - H = 0, \tag{21}$$

where λ is the London penetration depth having the following form:

$$\lambda^{-2}(T) = \frac{4\pi e^2}{c^2} \left(\frac{n_1(T)}{m_1} + 2\varepsilon_1 \left(n_1(T)\, n_2(T) \right)^{1/2} + \frac{n_2(T)}{m_2} \right). \tag{22}$$

It is well known that the lower critical field H_{c1} can be obtained in the same way as in Ref. [35]:

$$H_{c1} = \frac{\Phi_0}{4\pi\lambda^2(T)} \ln \kappa(T). \tag{23}$$

We then introduce a dimensionless lower critical field in the isotropic case $h_{c1} = H_{c1}(T)/H_{c1}(0)$, with

$$H_{c1}(0) = \frac{\Phi_0 e^2 T_c}{c^2} \left(\frac{\gamma_1}{\beta_1 m_1} + \frac{\gamma_2}{\beta_2 m_2} \right).$$

The normalized lower critical field is conveniently expressed by

$$h_{c1} = B(T) \ln \kappa(T), \tag{24}$$

where

$$B(T) = -\frac{2}{x + D^{-1}} \left[\varepsilon^2 + x(\tau - \tau_{c1})^2 + 2x\eta\varepsilon^2(\tau - \tau_{c1}) \right] \times \frac{\theta^2 + (2 - \tau_{c1} - \tau_{c2})\theta}{\varepsilon^2 D(\tau - \tau_{c2}) + (\tau - \tau_{c1})^3}, \tag{25}$$

$$D = \frac{\beta_1 \gamma_2^2}{\beta_2 \gamma_1^2}, \qquad \tau_{c1,c2} = \frac{T_{c1,c2}}{T_c}. \tag{26}$$

The temperature dependence of the normalized GL parameter $\kappa(T)$ in the two-band SC takes the form

$$\frac{\kappa(T)}{\kappa(0)} = \left(\frac{h_{c2}(T)}{B(T)} \right)^{1/2}. \tag{27}$$

Here, the upper critical field h_{c2} of two-band superconductors is given by expression (10).

2.4 Upper critical field H_{c2} of thin films

Let us assume now that the thickness of a two-band superconductor film is $d < \xi_{\text{eff}}, \lambda$, where the London penetration depth λ for two-band superconductors is defined by expression (22), and where $|\Psi_{10,20}(T)|^2$ is given by Eqns (6a), (6b). Then we may neglect variations in the order parameter in the film and suppose that a magnetic field penetrates the film almost completely. The surfaces of the film are recognized as coinciding with the planes $x = \pm d/2$. Neglecting the change in the order parameter in the thin film, Eqn (4a) can be rewritten as

$$\left(\frac{\hbar^2}{4m_1} - \frac{\varepsilon_1}{C}\right)\frac{x^2}{l_s^2}\,\Psi_1 + \left(\alpha_1(T) + \frac{\varepsilon}{C}\right)\Psi_1 + \beta_1\Psi_1^3 = 0\,. \quad (28)$$

Averaging the last expression over the thickness d of the film, we can obtain the dependence of the order parameter Ψ_1 on the applied magnetic field:

$$|\Psi_1|^2 = -\frac{1}{\beta_1}\left[\left(\alpha_1(T) + \frac{\varepsilon}{C}\right) + \left(\frac{\hbar^2}{4m_1} - \frac{\varepsilon_1}{C}\right)\frac{1}{l_s^4}\frac{d^2}{12}\right]. \quad (29)$$

Finally, using Eqns (9) and (29) we can deduce an equation for the upper critical field of the thin film:

$$\frac{d^2}{12(l_s^2)^2}\left[\frac{\hbar^2}{4m_1}\left(\frac{\hbar^2}{4m_2}\frac{1}{l_s^2} + \alpha_2\right) + \varepsilon_1\left(\varepsilon - \frac{\varepsilon_1}{l_s^2}\right)\right] + \left(\frac{\hbar^2}{4m_2}\frac{1}{l_s^2} + \alpha_2\right)\alpha_1 + \varepsilon\left(\varepsilon - \frac{\varepsilon_1}{l_s^2}\right) = 0\,. \quad (30)$$

In weak magnetic fields we obviously find

$$\frac{d^2}{12(l_s^2)^2}\left(\frac{\hbar^2}{4m_1}\alpha_2 + \varepsilon\varepsilon_1\right) + \left(\frac{\hbar^2\alpha_1}{4m_2} + \varepsilon\varepsilon_1\right)\frac{1}{l_s^2} + (\alpha_1\alpha_2 - \varepsilon^2) = 0\,. \quad (31)$$

The final expression for $H_{c2}^{\text{film}}(T)$ has the form [39]

$$H_{c2}^{\text{film}}(T) = -\frac{\hbar c}{2e}\left[-\left(\frac{\hbar^2\alpha_1}{4m_2} + \varepsilon\varepsilon_1\right) + \sqrt{\left(\frac{\hbar^2\alpha_1}{4m_2} + \varepsilon\varepsilon_1\right)^2 - 4(\alpha_1\alpha_2 - \varepsilon^2)\frac{d^2}{12}\left(\frac{\hbar^2}{4m_1}\alpha_2 + \varepsilon\varepsilon_1\right)}\right] \times \left[\frac{d^2}{6}\left(\frac{\hbar^2}{4m_1}\alpha_2 + \varepsilon\varepsilon_1\right)\right]^{-1}. \quad (32)$$

For thin films with $d \ll \xi_{\text{eff}}, \lambda$, we have

$$H_{c2}^{\text{film}}(T) = -\frac{\hbar c}{2e}\frac{\alpha_1(T)\,\alpha_2(T) - \varepsilon^2}{(\hbar^2/4)\left[\alpha_1(T)/m_2 + 4\varepsilon\varepsilon_1/\hbar^2\right]}\,. \quad (33)$$

2.5 Magnetization of two-band superconductors near H_{c2}

It is well known that the magnetization per unit volume in the case of single-band superconductors may be written as [35]

$$M(H,T) = -\frac{1}{4\pi}\frac{H_{c2}(T) - H}{(2\kappa^2 - 1)\,\beta_A}\,, \quad (34)$$

where κ is the GL parameter, and $\beta_A = 1.16$ for a triangular vortex lattice [35]. As follows from formula (34), the linearity of the experimentally examined $M(T)$ curves in single-band superconductors is the result of the linearity of the upper critical $H_{c2}(T)$ for a fixed value of the external magnetic field H and the temperature-independent character of the Ginzburg – Landau parameter κ. From Eqn (27) it follows that the magnetization exhibits a nonlinear character for the TB SC.

2.6 Flux quantization

This is a salient feature of a superconductor. It may be inferred by using Eqn (20) and assuming relationships (7). Proceeding as usual (see Ref. [35]), we arrive at

$$\mathbf{J} = \frac{2\pi}{\Phi_0}\left\{\frac{\hbar^2}{4m_1}n_1(T)\left(\frac{\mathrm{d}\phi_1}{\mathrm{d}\mathbf{r}} - \frac{2\pi\mathbf{A}}{\Phi_0}\right) + \frac{\hbar^2}{4m_2}n_2(T)\left(\frac{\mathrm{d}\phi_2}{\mathrm{d}\mathbf{r}} - \frac{2\pi\mathbf{A}}{\Phi_0}\right) + \varepsilon_1\left(n_1(T)\,n_2(T)\right)^{1/2}\cos(\phi_1 - \phi_2) \times \left[\left(\frac{\mathrm{d}\phi_1}{\mathrm{d}\mathbf{r}} - \frac{2\pi\mathbf{A}}{\Phi_0}\right) + \left(\frac{\mathrm{d}\phi_2}{\mathrm{d}\mathbf{r}} - \frac{2\pi\mathbf{A}}{\Phi_0}\right)\right]\right\}. \quad (35)$$

Let us now consider a hollow cylinder or, to put it differently, a tube with wall thickness larger than λ. We integrate this equation along a closed path lying entirely within the superconductor cavity in the cylinder. If the integration contour passes inside the wall, then $J = 0$ and the integral on the right-hand side is equal to zero. Taking into account relationships (7), we find that $\mathrm{d}\phi_1/\mathrm{d}\mathbf{r} = \mathrm{d}\phi_2/\mathrm{d}\mathbf{r}$. As a result, the magnetic field passing through the contour may take a discrete series of values Φ_0:

$$\Phi = n\Phi_0\,. \quad (36)$$

2.7 The Little – Parks effect in two-band superconductors

Let us take a thin cylindrical film where the thickness is much less than the penetration depth λ and apply a magnetic field along the axis of the cylinder. In this case, an SC cannot trap the magnetic flux because of its small thickness. However, the nonuniqueness of the phase leads to the oscillation of the critical temperature T_c with periodicity Φ_0 in the single-band approximation [35]. In a manner similar to that in the single-band superconductor case [35], using formula (19) and relationships (7a), (7b) as well as $\mathrm{d}\phi_1/\mathrm{d}r = \mathrm{d}\phi_2/\mathrm{d}r$, we can show that the critical temperatures in different bands vary as

$$T'_{c1} = T_{c1} - \frac{\hbar^2}{4m_1R^2\gamma_1}\left(n - \frac{\Phi}{\Phi_0}\right)^2, \quad (37a)$$

$$T'_{c2} = T_{c2} - \frac{\hbar^2}{4m_2R^2\gamma_2}\left(n - \frac{\Phi}{\Phi_0}\right)^2, \quad (37b)$$

where R is the radius of the cylinder. Then the critical temperature of the two-band superconducting cylinder is determined by the following expression [see also Eqn (11)]

$$(T_c - T'_{c1})(T_c - T'_{c2}) = \frac{\varepsilon'^2}{\gamma_1\gamma_2}\,, \quad (38)$$

where $\varepsilon' = \varepsilon + (\varepsilon_1/R^2)(n - \Phi/\Phi_0)^2$ [40].

2.8 Thermodynamic magnetic field $H_{cm}(T)$ and specific heat jump $\Delta C/C_N$

The free-energy difference between normal and superconducting states can be written down as

$$\Delta F = -\frac{\beta_1}{2}|\Psi_1|^4 - \frac{\beta_2}{2}|\Psi_2|^4 - 2\varepsilon|\Psi_1||\Psi_2|\,. \quad (39)$$

The last term in formula (39) is responsible for interband mixing and leads to an increase in free-energy differences and, consequently, in critical temperature. On the other hand, the thermodynamic magnetic field is related to the free-energy difference by

$$-\frac{H_{\rm cm}^2}{8\pi} = \Delta F\,. \tag{40}$$

In this paper we use the notation $H_{\rm cm}$ for the thermodynamic critical field of a bulky two-band superconductor, which is different from that for thin films. The calculated results for thin films are also important but are not considered here. Using formulas (6a), (6b), (39), and (40) as well as a series of appropriate manipulations, one can deduce the following formula for the thermodynamic magnetic field:

$$H_{\rm cm}(T) = -\sqrt{4\pi}\,\frac{\alpha_1(T)\,\alpha_2(T)-\varepsilon^2}{\varepsilon^2\beta_1\alpha_2(T)+\beta_2\alpha_1^3(T)} \times\left[\beta_1\varepsilon^4+\beta_2\alpha_1^4(T)-2\varepsilon^2\alpha_1(T)\,\frac{\varepsilon^2\beta_1\alpha_2(T)+\beta_2\alpha_1^3(T)}{\alpha_1(T)\,\alpha_2(T)-\varepsilon^2}\right]^{1/2}. \tag{41}$$

We now introduce a dimensionless parameter of the form

$$h_{\rm cm} = \frac{H_{\rm cm}(T)}{H_{\rm cm}(0)}\,,$$

where

$$H_{\rm cm}(0) = \sqrt{4\pi}\,T_{\rm c}\left(\frac{\gamma_1}{\beta_1^{1/2}}+\frac{\gamma_2}{\beta_2^{1/2}}\right),$$

and we then arrive at a normalized form of the thermodynamic magnetic field:

$$h_{\rm cm}(\theta) = -\frac{\sqrt{D}}{1+\sqrt{D}}\,\frac{1}{(\varepsilon^*)^2D(\tau-\tau_{\rm c2})+(\tau-\tau_{\rm c1})^3} \times\left[D(\varepsilon^*)^4+(\tau-\tau_{\rm c1})^4 - 2(\varepsilon^*)^2\,\frac{(\varepsilon^*)^2D(\tau-\tau_{\rm c2})+(\tau-\tau_{\rm c1})^3}{\theta^2+(2-\tau_{\rm c1}-\tau_{\rm c2})\theta}\right]^{1/2} \times\left[\theta^2+(2-\tau_{\rm c1}-\tau_{\rm c2})\theta\right], \tag{42}$$

where $(\varepsilon^*)^2 = \varepsilon^2/(\gamma_1\gamma_2T_{\rm c}^2)$. Here, notice that all the parameters are dimensionless and they are defined in formulas (10) and (26). With this result for the normalized field, we apply the Ruthgers formula to determining the specific heat jump at $T_{\rm c}$ for the two-band case:

$$\frac{\Delta C}{T_{\rm c}} = \frac{1}{4\pi}\left(\frac{\partial H_{\rm cm}}{\partial T}\right)^2_{T_{\rm c}}. \tag{43}$$

For the normalized specific heat jump at $T_{\rm c}$, we obtain [41]

$$\Delta c = \left(\frac{\partial h_{\rm cm}}{\partial\theta}\right)^2_{\theta=0}, \tag{44}$$

where

$$\Delta c = \frac{\Delta C}{\Delta C_0}\,,\qquad \frac{\Delta C_0}{T_{\rm c}} = \frac{1}{4\pi}\left(\frac{H_{\rm cm}(0)}{T_{\rm c}}\right)^2.$$

2.9 Critical current density $j_{\rm c}(T)$

It is well known that critical current density is defined by the expression [35]

$$j_{\rm c} = 2en_{\rm s}(T)\,v_{\rm c}(T)\,, \tag{45}$$

where $n_{\rm s}(T)$ is the superfluid density, and $v_{\rm c}(T)$ is the critical velocity of Cooper pairs. On the other hand, the superfluid density $n_{\rm s}(T)$ is related to the London penetration depth by the following formula [35]

$$\frac{n_{\rm s}(T)}{n_{\rm s}(0)} = \frac{\lambda^2(0)}{\lambda^2(T)}\,. \tag{46}$$

The London penetration in the framework of the TB GL theory is given by expression (22). The critical velocity of Cooper pairs $v_{\rm c}$ is determined by the coherence length:

$$v_{\rm c} = \frac{2\hbar}{m_0\xi(T)}\,, \tag{47}$$

where m_0 is the effective mass of a Cooper pair, and the coherence length is given by

$$\xi^2(T) = \frac{\Phi_0}{2\pi H_{\rm c2}}\,. \tag{48}$$

As a result of calculations we can get the final expression for normalized critical current density [42]:

$$\frac{j_{\rm c}(T)}{j_{\rm c}(0)} = \frac{\lambda^2(0)}{\lambda^2(T)}\left(h_{\rm c2}(T)\right)^{1/2}. \tag{49}$$

2.10 Effects of anisotropy on the upper critical field

Results presented in Sections 2.1 – 2.4, 2.9 are suitable for explaining experimental data of bulky polycrystalline samples. Recent studies concerning the growth of single-crystal magnesium diboride MgB_2 [43, 44] showed anisotropy of its physical properties. The mass anisotropy parameter $\gamma = (m^c/m^{ab})^{1/2}$ of MgB_2 in the literature ranges from 1.2 to 9 in polycrystalline samples, and 4.31 – 4.36 in single crystals [43]. From this point of view, derivations and calculations in the framework of the anisotropic two-band Ginzburg – Landau model seem attractive. The SB s-wave GL theory for layered superconductors was developed in works [45 – 47].

One can write the TB GL functional for layered superconductors in the form

$$F[\Psi_{1n},\Psi_{2n}] = \sum_n\int {\rm d}^2r\left(F_{1n}+F_{1n,2n}+F_{2n}+F_{1n,1(n+1)} + F_{2n,2(n+1)}+\frac{H^2}{8\pi}\right), \tag{50}$$

where

$$F_{in} = \frac{\hbar^2}{4m_i^{ab}}\left|\left(\nabla_{\rm 2d}-\frac{2\pi{\rm i}\mathbf{A}}{\Phi_0}\right)\Psi_{in}\right|^2+\alpha_{in}(T)\Psi_{in}^2+\frac{\beta_{in}}{2}\,\Psi_{in}^4\,, \tag{51}$$

$$F_{1n,2n} = \varepsilon(\Psi_{1n}\Psi_{2n}^*+{\rm c.c.}) + \varepsilon_1\left[\left(\nabla_{\rm 2d}+\frac{2\pi{\rm i}\mathbf{A}}{\Phi_0}\right)\Psi_{1n}^*\left(\nabla_{\rm 2d}-\frac{2\pi{\rm i}\mathbf{A}}{\Phi_0}\right)\Psi_{2n}+{\rm c.c.}\right], \tag{52}$$

$$F_{in,i(n+1)} = \frac{\hbar^2}{4m_i^cd^2}\left|\Psi_{in}-\Psi_{i(n\pm1)}\exp\left(-{\rm i}\,\frac{2\pi dA_z}{\Phi_0}\right)\right|^2, \tag{53}$$

and d is the distance between planes. We choose x, y, z axes lying along the a, b, and c crystallographic axes, respectively. Due to the identical character of the planes we can write $\alpha_{in} = \alpha_i$, $\beta_{in} = \beta_i$. The choice of the vector-potential $\mathbf{A}$ in the form of $\mathbf{A} = (0, Hx, 0)$ corresponds to the perpendicular component of the magnetic field $\mathbf{H} = (0, 0, H)$. In this case, GL equations for TB layered superconductors can be reduced to Eqns (8a), (8b). Calculation of $H_{c2}^{\perp}$ leads to the result

$$H_{c2}^{\perp}(T) = \frac{\Phi_0}{2\pi\xi_{\perp}^2}\,, \tag{54}$$

where the effective coherence length ξ_{eff} of two-band superconductors is defined by the expression

$$\xi_{\perp}^2 = \frac{\hbar^2}{4}\left\{-\left(m_1\alpha_1(T) + m_2\alpha_2(T) + \frac{8\varepsilon\varepsilon_1 m_1 m_2}{\hbar^2}\right) + \left[\left(m_1\alpha_1(T) + m_2\alpha_2(T) + \frac{8\varepsilon\varepsilon_1 m_1 m_2}{\hbar^2}\right)^2 - 4m_1 m_2\left(\alpha_1(T)\,\alpha_2(T) - \varepsilon^2\right)\right]^{1/2}\right\}^{-1}. \tag{55}$$

At small values of the upper critical field $H_{c2}^{\perp}(T)$, the following relationship is valid:

$$H_{c2}^{\perp}(T) = -\frac{\hbar c}{2e}\,\frac{\alpha_1(T)\,\alpha_2(T) - \varepsilon^2}{(\hbar^2/4)\left[\alpha_1(T)/m_2 + \alpha_2(T)/m_1 + 8\varepsilon\varepsilon_1/\hbar^2\right]}\,. \tag{56}$$

For the calculation of $H_{c2}^{\parallel}$, we choose $\mathbf{H} = (0, H, 0)$ and $\mathbf{A} = (0, 0, -Hx)$. Then GL equations for TB superconductors are reduced to the following forms

$$-\frac{\hbar^2}{4m_1}\frac{\mathrm{d}^2\Psi_1}{\mathrm{d}x^2} + \alpha_1\Psi_1 + \varepsilon\Psi_2 + \varepsilon_1\frac{\mathrm{d}^2\Psi_2}{\mathrm{d}x^2} + 2\,\frac{\hbar^2}{4m_1^c d^2}\left(1 - \cos\frac{2\pi dHx}{\Phi_0}\right)\Psi_1 = 0\,, \tag{57a}$$

$$-\frac{\hbar^2}{4m_2}\frac{\mathrm{d}^2\Psi_2}{\mathrm{d}x^2} + \alpha_2\Psi_2 + \varepsilon\Psi_1 + \varepsilon_1\frac{\mathrm{d}^2\Psi_1}{\mathrm{d}x^2} + 2\,\frac{\hbar^2}{4m_2^c d^2}\left(1 - \cos\frac{2\pi dHx}{\Phi_0}\right)\Psi_2 = 0\,. \tag{57b}$$

By elimination of unknowns we can get equations for Ψ_1 and Ψ_2 from Eqns (57a) and (57b), which turn out to be identical:

$$\frac{\hbar^2}{4m_1}\frac{\hbar^2}{4m_2}\frac{\mathrm{d}^4\Psi_1}{\mathrm{d}x^4} - \left(\frac{\hbar^2}{4m_2}\alpha_1 + \frac{\hbar^2}{4m_1}\alpha_2\right)\frac{\mathrm{d}^2\Psi_1}{\mathrm{d}x^2} + \alpha_1\alpha_2\Psi_1 + \left(1 - \cos\frac{2\pi dHx}{\Phi_0}\right)\left(2\,\frac{\hbar^2}{4m_1^c d^2}\left[-\frac{\hbar^2}{4m_2}\frac{\mathrm{d}^2}{\mathrm{d}x^2} + \alpha_2\right] + 2\,\frac{\hbar^2}{4m_2^c d^2}\left[-\frac{\hbar^2}{4m_1}\frac{\mathrm{d}^2}{\mathrm{d}x^2} + \alpha_1\right]\right)\Psi_1 = \left(\varepsilon^2 + 2\varepsilon\varepsilon_1\frac{\mathrm{d}^2}{\mathrm{d}x^2} + \varepsilon_1^2\frac{\mathrm{d}^4}{\mathrm{d}x^4}\right)\Psi_1\,. \tag{58}$$

By neglecting high derivatives of the order parameter, $\mathrm{d}^4\Psi_1/\mathrm{d}x^4$, and small terms, we can obtain the Mathieu equation for the calculation of the upper critical field $H_{c2}^{\parallel}$:

$$-\left(\frac{\hbar^2}{4m_2}\alpha_1 + \frac{\hbar^2}{4m_1}\alpha_2 + 2\varepsilon\varepsilon_1\right)\frac{\mathrm{d}^2\Psi_1}{\mathrm{d}x^2} + 2\left(\frac{\hbar^2}{4m_1^c d^2}\alpha_2 + \frac{\hbar^2}{4m_2^c d^2}\alpha_1\right)\left(1 - \cos\frac{2\pi dHx}{\Phi_0}\right)\Psi_1 = (\varepsilon^2 - \alpha_1\alpha_2)\Psi_1\,. \tag{59}$$

In weak magnetic fields $H \ll \Phi_0/(2\pi d^2)$, and after expansion of cosines in Eqns (57a), (57b), we can get the final expression for the anisotropy parameter of the upper critical field:

$$\gamma_{H_{c2}} = \frac{H_{c2}^{\parallel}}{H_{c2}^{\perp}} = \left[\frac{x(T - T_{c1}) + (T - T_{c2}) + 8\varepsilon^2 x\eta T_c}{(m_2/m_2^c)\,x(T - T_{c1}) + (m_1/m_1^c)(T - T_{c2})}\right]^{1/2}. \tag{60}$$

In strong magnetic fields $H > \Phi_0/(2\pi d^2)$, the upper critical field $H_{c2}^{\parallel}$ can be determined from the lowest eigenvalue of the Mathieu equation [48] and is given by the following expression [49]

$$H_{c2}^{\parallel} = \frac{\Phi_0}{2\pi d}\left(\alpha_2\frac{\hbar^2}{4m_1^c d^2} + \alpha_1\frac{\hbar^2}{4m_2^c d^2}\right) \times \left[\left(\frac{\hbar^2}{4m_2}\alpha_1 + \frac{\hbar^2}{4m_1}\alpha_2 + 2\varepsilon\varepsilon_1\right) \times \left(\alpha_2\frac{\hbar^2}{4m_2^c d^2} + \alpha_1\frac{\hbar^2}{4m_1^c d^2} - \frac{\varepsilon^2 - \alpha_1\alpha_2}{2}\right)\right]^{-1/2}. \tag{61}$$

This means that

$$H_{c2}^{\parallel} < \frac{1}{(T - T^*)^{1/2}}\,, \tag{62}$$

where

$$T^* = T_c - \frac{\hbar^2}{4m_1^c d^2\gamma_1} - \frac{\hbar^2}{4m_2^c d^2\gamma_2}\,. \tag{63}$$

A similar calculation in the framework of the above-considered TB GL theory using the anisotropic mass tensor method was carried out in the quite recent paper [50].

2.11 Effects of anisotropy on London penetration depth λ

Using equations (20), (21) in the case of $\mathbf{H} = (0, 0, H)$ we can show that the London penetration depth $\lambda_{\perp}$ perpendicular to superconducting layer is determined by expression (22). For the calculation of $\lambda_{\parallel}$, we choose $\mathbf{H} = (0, H, 0)$ and $\mathbf{A} = (0, 0, -Hx)$. Taking into account the equilibrium value of the phase difference ($\phi_{in} - \phi_{i(n\pm g)} = 2\pi n$) we can get the equation for the vector-potential:

$$\frac{\mathrm{rot}\,\mathrm{rot}\,\mathbf{A}}{4\pi} = \frac{2\pi}{\Phi_0}\left\{\frac{\hbar^2}{4m_1^c d}\,n_1(T) + \frac{\hbar^2}{4m_2^c d}\,n_2(T)\right\} \times \sin\left(\frac{2\pi}{\Phi_0}A_z d\right)\mathbf{n}_z\,, \tag{64}$$

where $\mathbf{n}_z$ is a unit vector in the z-direction.

In weak magnetic fields $H \ll \Phi_0/(2\pi d^2)$, and after expansion of the sine in Eqn (64) and applying the Maxwell equation, we can get the final expression for the magnetic

field, which is the same as Eqn (21) with the replacement of

$$\lambda_{\parallel}^{-2}(T) = \frac{4\pi e^2}{c^2}\left\{\frac{n_1(T)}{m_1^c} + \frac{n_2(T)}{m_2^c}\right\}. \quad (65)$$

Correspondingly, we obtain the following expression for the anisotropy parameter $\gamma_\lambda = \lambda_\parallel/\lambda_\perp$ of London penetration depth:

$$\gamma_\lambda = \frac{n_1(T)/m_1 + 2\varepsilon_1\big(n_1(T)\,n_2(T)\big)^{1/2} + n_2(T)/m_2}{n_1(T)/m_1^c + n_2(T)/m_2^c}. \quad (66)$$

Generally, without expansion of the sines and for a strong magnetic field of $H > \Phi_0/(2\pi d^2)$, Eqn (64) has a solution corresponding to a single vortex directed parallel to the superconducting layer. In this case, the boundary condition requires that the total magnetic field flux through the yz-plane be equal to the magnetic flux quantum Φ_0. The angular dependence of a magnetic field in a vortex also seems interesting. The existence of the second order parameter can lead to an additional angular dependence of the magnetic field in a vortex. Using the solution of the Ferrell–Prange equation [35] for the vector-potential A, we can demonstrate that the expression for the London penetration depth remains the same as in formula (65). This means that the temperature-dependent anisotropy γ_λ of the London penetration depth, defined by expression (66), is valid in all magnetic fields.

3. Results and discussion

3.1 Upper critical field $H_{c2}(T)$

The experimental data for the upper critical field h_{c2} of MgB_2, $LuNi_2B_2C$, and YNi_2B_2C compounds can be described with high accuracy by the simple expression

$$h_{c2}(\theta) = \frac{H_{c2}}{H_{c2}^*(0)} = \frac{(-\theta)^{1+\alpha}}{1-(1+\alpha)w + lw^2 + mw^3}, \quad (67)$$

where $w = (1+\theta)(-\theta)^{1+\alpha}$. This formula was applied by Drechsler et al. [51] to fitting the experimental data on h_{c2} in nonmagnetic borocarbides. The critical exponent α defines the temperature dependence more effectively, being very sensitive to disorder, i.e. to the quality of the samples. With increasing disorder the positive curvature and, correspondingly, α decrease [19]. The saturation (negative curvature) at low temperatures is well described by the ratio l/m, which is assumed by analogy to be sensitive to the electronic structure. For $l > m$, the temperature range with negative curvature widens. For $l < m$, we have an upper critical field changing almost linearly with temperature.

In Fig. 1 we plotted the experimental data by Freudenberger et al. [19] for the upper critical field $H_{c2}(T)$ in $LuNi_2B_2C$ versus the reduced temperature T/T_c, and also showed the theoretical fits with this data by using formulas (10) and (67). The best fit with the experimental data was obtained by using formula (67) (shown by the dashed line) with fitting parameters $\mu_0 H_{c2}^*(0) = 7.75$ T, $\alpha = 0.24$, $l = 3$, and $m = -1$. The solid line in Fig. 1 displays the results of two-band GL fitting by using formulas (10). For this fitting, the GL parameters, together with other fitting parameters, were $A = 0.66$, $B = -0.03$, $c_0 = 0.19$, $x = 5$, $\mu_0\tilde{H}_{c2}(0) = 7.02$ T, $T_{c1} = 9.8$ K, and $T_{c2} = 2.3$ K.

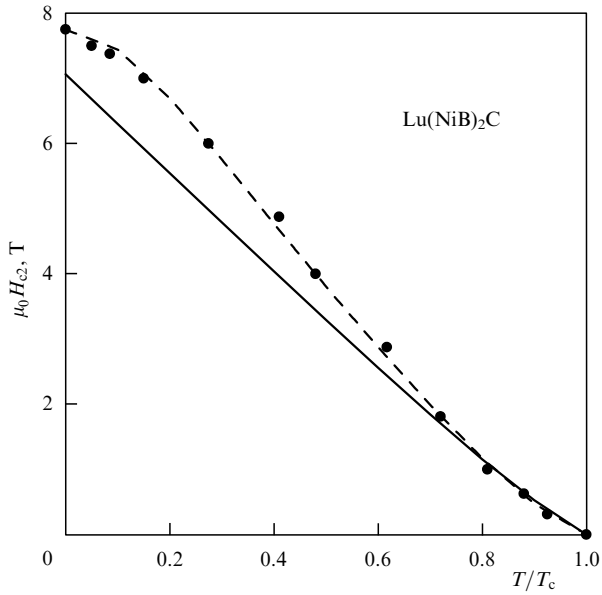

Figure 1. Dependence of the upper critical field $H_{c2}(T)$ for $LuNi_2B_2C$ versus reduced temperature T/T_c. The black circles show the experimental data [19], while the solid line is for the GL theoretical expectations of $H_{c2}(T)$. The dashed line corresponds to calculations with the fitting formula (67).

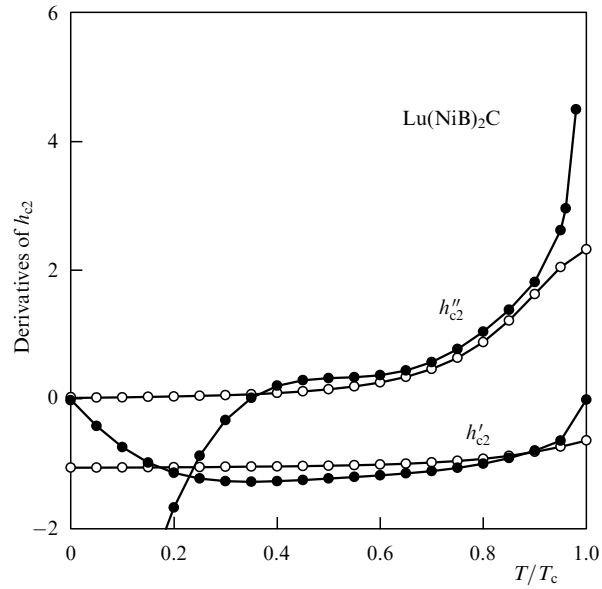

Figure 2. The first and second derivatives of quantities defined by equations (10) and (67) versus reduced temperature T/T_c for $LuNi_2B_2C$. The white circles show the derivatives calculated using GL equations (10), while the black circles show the fitting formula (67) derivatives.

In Fig. 2 we plotted the first and second derivatives of h_{c2} with respect to reduced temperature T/T_c in $LuNi_2B_2C$ using formulas (10) and (67). The two-band GL theory (white circles) yields a negative first derivative below T_c. On the other hand, the first derivative of the fitting formula (67) (black circles) starts from zero at absolute zero of temperature, goes through a negative region, and returns to zero at T_c. There is good agreement in the temperature range from $0.4T_c$ to $0.95T_c$. The plots of the second derivatives are also presented in the same figure. Good agreement in the same temperature range is observed for the second derivatives, too.

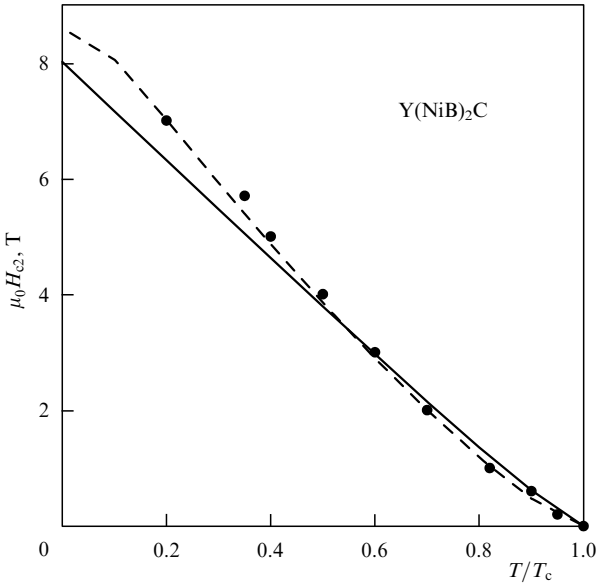

Figure 3. Dependence of the upper critical field $H_{c2}(T)$ for YNi_2B_2C versus reduced temperature T/T_c. Black circles show the experimental data [20], while the solid line is the GL theoretical expectations of $H_{c2}(T)$. The dashed line corresponds to calculations with the fitting formula (67).

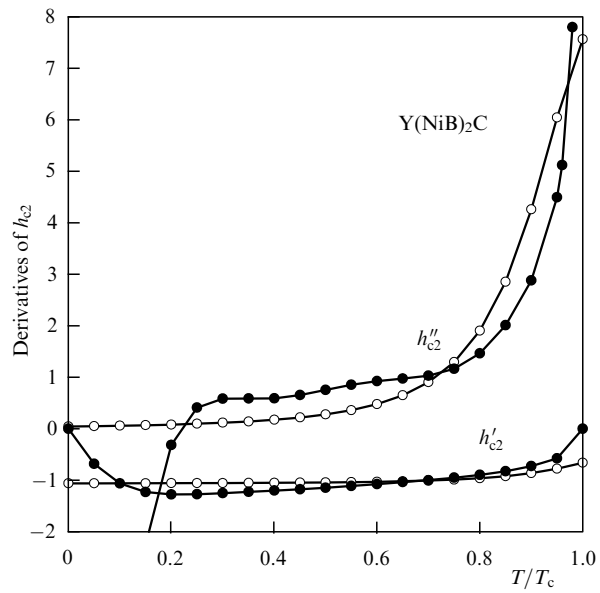

Figure 4. The first and second derivatives of quantities defined by equations (10) and (67) versus reduced temperature for YNi_2B_2C. The white circles show the derivatives calculated using GL equations (10), while the black circles show the fitting formula (67) derivatives.

The fitted results for YNi_2B_2C are presented in Figs 3 and 4. We utilized the following values of the parameters [20]: $\mu_0 H^*_{c2}(0) = 8.6$ T, $\alpha = 0.28$, $l = 7$, and $m = -13$, while for the GL set of parameters we resorted to $A = 0.71$, $B = -0.044$, $c_0 = 0.157$, $x = 5$, $\mu_0 \tilde{H}_{c2}(0) = 8$ T, $T_{c1} = 10$ K, and $T_{c2} = 1.825$ K. Similar calculations for the bulky MgB_2 using Eqns (10) and (67) have been done in Ref. [32] and good agreement with experimental data [21, 22] have been achieved.

In the case of no intergradient interaction of order parameters ($\eta = 0$), the GL curvature reaches its maximum at the point $\theta = B/(2A) = 0.5$. The inclusion of a negative intergradient interaction shifts this maximum to the region close to critical temperature. Physically, this means that in the vicinity of T_c, when both order parameters are small, their interaction becomes important for the behavior of the upper critical field. As shown by relationship (11), the critical temperature of about $T_c = 16$ K can be obtained from $T_{c1} = 9.8$ K and $T_{c2} = 2.3$ K with the interaction parameter equal approximately to 0.33 in the case of the $LuNi_2B_2C$ compound. In the case of YNi_2B_2C, the following parameters have been used: $T_{c1} = 10$ K, $T_{c2} = 1.825$ K, and 0.33 for the interaction parameter. It should be emphasized that we must take two rather different critical temperatures, $T_{c1} \gg T_{c2}$, in contrast to similar calculations for MgB_2 [32].

The upper critical field h_{c2} is governed by the parameters ε and ε_1. As follows from expression (10), the upper critical field is determined mainly by the larger mass m_1, while the contribution from the smaller mass can be neglected in the case of two different effective masses. In calculating mass ratio parameter x for $LuNi_2B_2C$ and YNi_2B_2C borocarbides, we set the Fermi velocity in different bands equal to $v_{F1} = 0.85 \times 10^7$ cm s^{-1}, $v_{F2} = 3.8 \times 10^7$ cm s^{-1} [23]. This leads to the mass ratio parameter x being taken as 5, while for MgB_2 x is equal to 3 [32, 33].

Notice that the discordance between theory and experiment comes into prominence at temperatures very close to T_c (see Figs 2 and 4). It seems likely that we have two main reasons for the mismatch between theory and experiment at these temperatures. First, the thermal fluctuations may increase the positive curvature near T_c, which are ignored in the GL theory entering the class of mean field theories. Fluctuations might be strongly enhanced due to the nested regions on the Fermi surface, which contribute significantly to the group of slow electrons described within our two-band model [13]. Second, in the calculations, we resorted to a linear two-band GL theory for which there exist analytical solutions. For a better fit, the cubic terms must be included in the two-band GL theory. Then the equations to be solved would necessitate solutions for the vortex state and its symmetry in the two-band GL theory.

3.2 Surface critical field $H_{c3}(T)$

From Eqn (18) one can see that the surface critical field $H_{c3}(T)$ possesses the temperature dependence similar to those of $H_{c2}(T)$ for both single-band and two-band GL models. The appropriate calculations favor the existence of the surface critical field. The first angle-resolved photoemission spectroscopy measurements on an MgB_2 single crystal were reported by Uchiyama et al. [52]. They observed several surface states. The effect of the surface states on the superconductivity has been discussed in Ref. [53]. The authors reasoned that the surface critical magnetic field does not exist and that the surface electronic states can be responsible for the nonexistence of the surface critical field. As mentioned in this paper, no H_{c3} has been observed in nonmagnetic borocarbides. However, Welp et al. [54] presented data on $H_{c3}(T)$ for an MgB_2 single crystal very recently. In their c-axis measurements, the surface critical field features a linear dependence, whereas it has a positive curvature for ab-plane measurements. It should be noted that anisotropy shows itself in the measurements. However, the calculations also presented here take advantage of isotropic superconductivity for the two-band GL theory. Although the influence of the surface states on superconductivity is still controversial, it has been suggested that

superconductivity is suppressed on *ab*-surfaces, while it is unaffected along the *c*-axis.

According to our calculations in the framework of the isotropic TB GL theory, the upper critical field reveals positive curvature at temperatures close to T_c. With the parameters of TB GL theory presented in Ref. [32] one can examine experimentally a surface critical field H_{c3} with a positive curvature similar to that for H_{c2} in a bulky MgB_2 superconductor. In our opinion, the preparation of bulk samples with smooth and clean surfaces would be enough for taking the measurements in MgB_2. The paramagnetic Meissner effect associated with the existence of the surface critical field was observed for the first time in finite-sized MgB_2 pellets and superconducting cores of iron-sheathed MgB_2 tubes in Ref. [55]. The paramagnetic Meissner effect can be attained in the framework of the self-consistent solution of single-band GL equations for a cylinder of a finite size [56]. The surface magnetic field in dirty two-band superconductors was calculated in Ref. [57] using the BCS theory. It was shown that interaction of the two bands leads to a novel scenario, with the ratio H_{c3}/H_{c2} varying with temperature. The results were applied to MgB_2, and the ratio turned out to be less than 1.6946.

3.3 Lower critical field $H_{c1}(T)$

In Fig. 5, we plotted $h_{c1}(T)$ as a function of the reduced temperature T/T_c. Ghosh et al. [58] found that the lower critical field of YNi_2B_2C borocarbides follows a power law dependence of the form $h_{c1} = H_{c1}/H_{c1}^*(0) = 1 - (T/T_c)^2$, with $H_{c1}^*(0) = 22$ mT. The black circles in the graph in Fig. 5 depict their results. To our best knowledge, no measurements of the lower critical field for $LuNi_2B_2C$ have ever been made. The line exhibits the results of calculations done in the context of the two-band GL theory. Here, we utilized expressions (10), (24), and (27) with the parameter $D = 1.5$. The rest of the GL parameter set was similar to that used to determine the temperature dependence of the upper critical field h_{c2} in YNi_2B_2C (see Section 3.1). The temperature dependence of

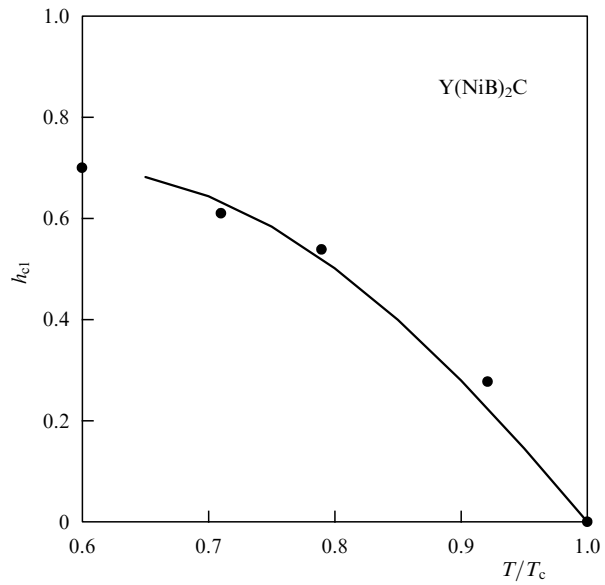

Figure 5. Dependence of the lower critical field $H_{c1}(T)$ for YNi_2B_2C versus reduced temperature T/T_c. Black circles show the experimental data [58], while the solid line corresponds to the GL theoretical expectations of $H_{c1}(T)$.

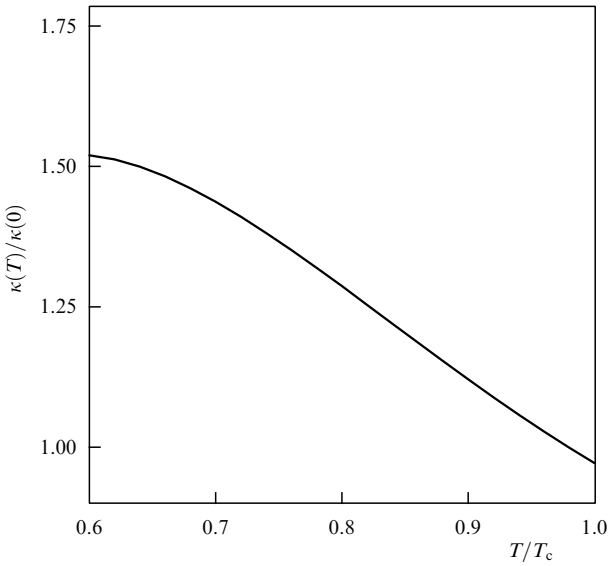

Figure 6. Dependence of the GL parameter for YNi_2B_2C versus reduced temperature T/T_c, based on Eqn (27).

the GL parameter $\kappa(T)$, obtained from Eqn (27) with the same fitting parameters, is presented in Fig. 6. As shown in the figure, $\kappa(T)$ varies slowly with temperature and, as a result, the temperature dependence of h_{c1} in Eqn (22) is mainly determined by the London penetration depth $\lambda(T)$. Calculations of h_{c1} for magnesium diboride MgB_2 using the TB GL theory were carried out in Ref. [33], and good agreement has also been achieved.

It should be noted that the temperature dependence h_{c1} in the two-band GL theory is predominantly determined by the interaction parameters ε and ε_1. When the carriers have various effective masses in different bands ($m_1 \gg m_2$), the lower critical field h_{c1} can more effectively be determined by the small mass, in contrast to the upper critical field. The contribution from the larger mass can be neglected in such a case. As shown in Fig. 5, the theoretical data of the two-band GL theory are in good agreement with available experimental data [58].

3.4 Upper critical field H_{c2} of thin films

As follows from formula (32), the upper critical field of the thin film of two-band superconductors increases as d^{-2} with decreasing film thickness. It is well known that $H_{c2}^{\text{film}}(T)$ for single-band superconducting films increases as d^{-1} [35]. The common feature of expressions (10) and (33) is the presence of positive curvature at critical temperature T_c for bulk samples and films. Such a conclusion is in agreement with experimental data for bulk samples of nonmagnetic borocarbides and magnesium diboride [32, 33], and for MgB_2 thin films [59].

Using expression (32) we can calculate the slope angle of the upper critical field in bulk and thin-film samples at T_c. For the estimation of the ratio of slopes at T_c, namely

$$\frac{\mathrm{d}H_{c2}^{\text{film}}(T)/\mathrm{d}T}{\mathrm{d}H_{c2}^{\text{m}}(T)/\mathrm{d}T},$$

we can draw on Eqns (30)–(33) with the parameters which were also used in Refs [32, 33] when determining the temperature dependences of different physical quantities for

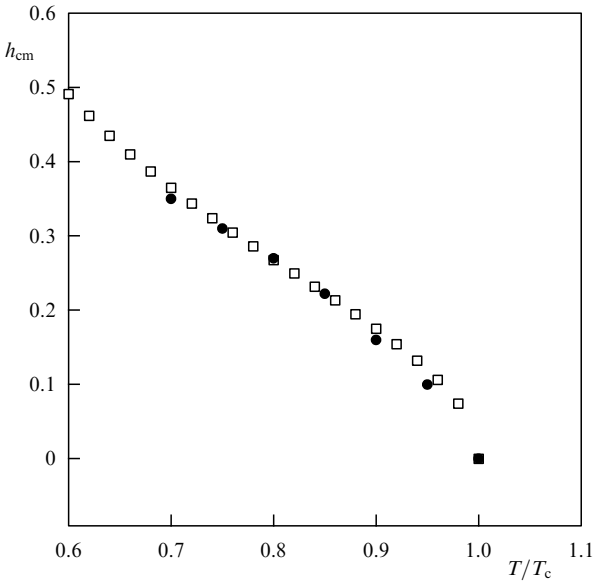

Figure 7. Temperature dependence of the thermodynamic magnetic field for MgB_2.

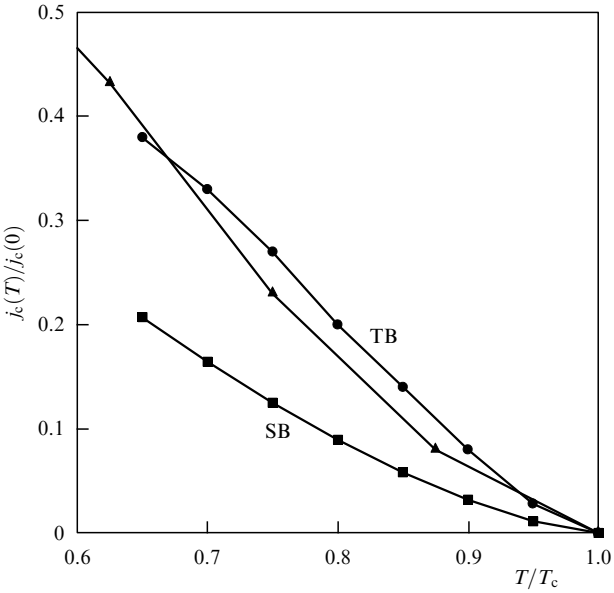

Figure 8. Temperature dependence of the critical current density for MgB_2 (black circles are the results of the two-band GL theory; black squares are the results of the single-band GL model; black triangles represent experimental data [70]).

bulk MgB_2 samples. With this choice of parameters, the ratio of slopes at T_c, i.e.

$$\frac{dH_{c2}^{\text{film}}(T)/dT}{dH_{c2}^{\text{m}}(T)/dT},$$

is equal approximately to 1.65. As follows from Refs [59 – 62], the ratio of slopes for bulk samples and thin films varies over the interval 1.5 – 2.2.

3.5 Magnetization $M(T)$

The temperature dependence of $H_{c2}(T)$ near T_c exhibits a positive curvature, implying that the temperature dependence of the magnetization of two-band superconductors near $H_{c2}(T)$ demonstrates nonlinear behavior at a fixed external magnetic field. Nonlinear magnetization of MgB_2 in the vicinity of $H_{c2}(T)$ was reported in Ref. [28], and more recently in Ref. [63]. The temperature variation in the GL parameter κ leads to changing the type of superconductor from type II to type I in the vicinity of the critical temperature. Similar effects in cuprate superconductors were discussed recently by Landau and Ott [64].

3.6 Flux quantization

Experiments with quantum interference devices based on MgB_2 were reported in Refs [65, 66]. As follows from relationship (36), quantization of the magnetic flux in two-band SCs remains the same as in the single-band case. The results of these experiments [65, 66] confirms the flux quantization phenomenon (36).

3.7 The Little – Parks effect

As follows from expression (38), due to different periods of oscillations of critical temperature in different bands (37a), (37b), periodicity in changing T_c of a two-band superconductor is absent, in contrast to single-band superconductors. Unfortunately, no experimental data on the Little – Parks effect are available in two-band MgB_2, $LuNi_2B_2C$, or YNi_2B_2C superconductors.

3.8 Thermodynamic magnetic field $H_{cm}(T)$ and $\Delta C/C_N$

It should be emphasized that the thermodynamic magnetic field $H_{cm}(T)$ does not comprise a directly measurable quantity. Fortunately, it can be calculated from specific heat measurements. In Fig. 7, we plotted the temperature dependence of $H_{cm}(T)$ in MgB_2, calculated using formula (42) (circles). To produce the data for Fig. 7, we have employed the same parameters as in Refs [32, 33]. Empirical data for h_{cm} (squares) were extracted from the results of Bouquet et al. [10] with $H_{cm}^*(0) = 0.36$ T. Similar results were also obtained experimentally in the work by Wang et al. [28].

Substituting a calculated value of $\partial h_{cm}/\partial\theta$ at the critical temperature into Eqn (44), we can estimate the specific heat jump at T_c. The estimated value for the jump was found to be 0.64, which is small compared to the value of unity calculated in the single-band GL theory. However, this value is consistent with the experimental data obtained in Ref. [10], according to which $\Delta C/C_N = 0.8$ is smaller than the single-band BCS value of 1.43. Analogous reduction in the specific heat jump was revealed by two-band BCS calculations which were conducted by Moskalenko et al. [67] and more recently in Refs [68, 69].

3.9 Critical current density $j_c(T)$

Figure 8 displays the critical current density (49) as compared with that given by the single-band Ginzburg – Landau model [35]: $j_c(T)/j_c(0) = (1 - T/T_c)^{3/2}$. It is easily seen that both curves exhibit positive curvature of critical current density at T_c. The triangles show the experimental data of recent measurements in Ref. [70]. It is apparent that the TB GL theory gives a good approximation to the experimental data [70] (see also review [71]).

3.10 H_{c2} anisotropy effects

Experimental studies of the anisotropy of the superconducting state properties in MgB_2 were recently conducted [72 – 74]. In Fig. 9, we plotted anisotropy parameter γ versus reduced temperature T/T_c. Experimental results by Lyard et

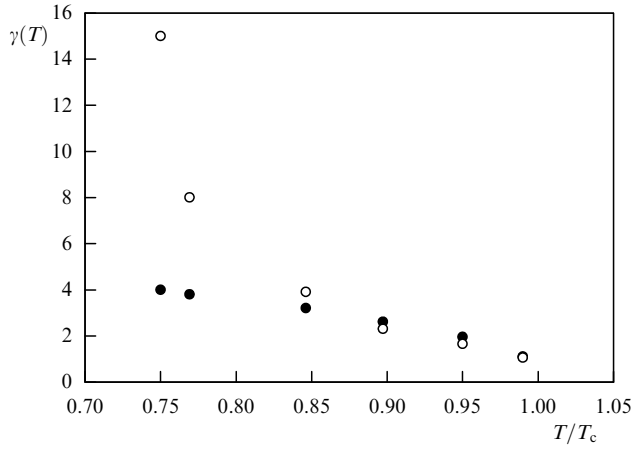

Figure 9. Temperature dependence of the anisotropy parameter for MgB_2 single crystals (black circles are experimental data taken from Ref. [73]; white circles are the results of the anisotropic TB GL theory).

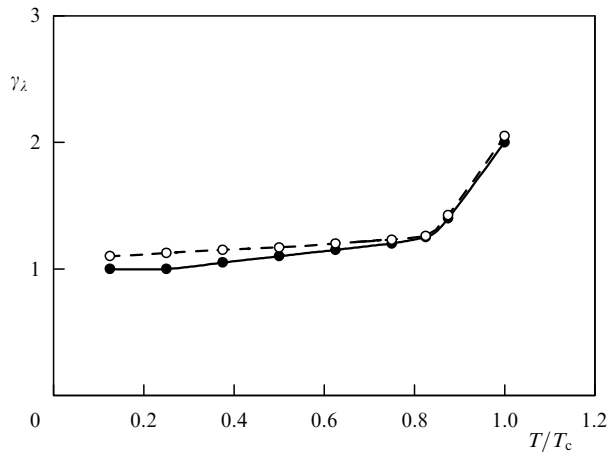

Figure 10. Temperature dependence of the anisotropy parameter of the London penetration depth for MgB_2 single crystals (black circles are experimental data taken from Ref. [86]; white circles are the results of analysis using the anisotropic TB GL theory).

al. [73] are marked by the black circles. The white circles denote the results of calculations from the above-presented TB GL theory for layered superconductors. The same values of the parameters were also utilized in Refs [32, 33] for determining the temperature dependence of SC state parameters in the framework of the isotropic TB GL theory. Anisotropy mass parameters for single crystals ($m_2/m_2^c = 1.3$ and $m_1/m_1^c = 0.03$) are the same as in Ref. [75]. As follows from formula (60), the influence of a π (weak) band is effectively 'switched off' and the anisotropy parameter is mainly determined by the σ (strong) band. As a consequence, at a small magnetic field there is a good agreement with experimental data on investigation of the upper critical field anisotropy. An increase in γ with decreasing temperature has been examined experimentally by many groups [77, 78]. Thus, there is a consensus for understanding the temperature behavior of γ in SCs.

In a high magnetic field, $H_{c2}^{\parallel}$ goes to infinity as $(T - T^*)^{1/2}$. This means that the orbital depairing effect of a magnetic field parallel to the layers does not destroy the superconductivity. This corresponds to the case where the cores of the vortices reside between the SC layers and the external magnetic field has no influence on the superconductivity. In fact, other magnetic mechanisms can restrict the divergence. The divergence of $H_{c2}^{\parallel}$ at T^* is removed by taking into account spin – orbit scattering [79] and the paramagnetic effect [80, 81]. An analogous anisotropy of the upper critical field was observed for the other possible class of two-band superconductors — nonmagnetic $Y(Lu)Ni_2B_2C$ borocarbides [82].

Here, it is necessary to remark that similar two-band GL equations were recently analyzed in Refs [83, 84]. However, terms similar to the intergradient interaction terms in Eqns (4a), (4b) and (8a), (8b) are absent in equations presented in Refs [83, 84]. As shown in Refs [32, 33], maximum positive curvature of the upper critical field in bulky samples can be achieved by the inclusion of an intergradient interaction. In the case of no intergradients of order parameters ($\eta = 0$), the curvature reaches a maximum at the point $0.5T_c$. Intergradient interaction shifts this maximum to the region close to the critical temperature. Such a behavior is in good agreement with experimental data for bulky samples. As we can see from expression (60), in the case of anisotropic GL equations, the intergradient interaction term also plays a crucial role in the temperature dependence of the anisotropy parameter $\gamma_{H_{c2}}$.

Another version of the GL approximation was presented in Ref. [85]. This approach corresponds to an effective single-band GL theory. In the framework of theory [85], the ratio of order parameters is temperature- and field-independent, i.e., it is constant, meaning that the two-band GL theory is equivalent to the effective single-band approximation. In contrast to Ref. [85], in our consideration the ratio of order parameters is temperature- and field-dependent [see also Eqns (4a), (4b) and (8a), (8b)].

3.11 λ anisotropy effects

In Fig. 10, we plotted anisotropy parameter γ_λ versus reduced temperature T/T_c. Experimental data obtained by Lyard et al. [86] are given by the black circles. The white circles denote the results of calculations using Eqns (6a), (6b), and (66). Due to negative sign of the intergradient interaction η, the anisotropy factor γ_λ of the London penetration depth reduces with decreasing temperature. Similar experimental results were also obtained by Cubitt et al. [87] and Zehetmayer et al. [44].

In papers [75, 76], the anisotropy parameters of H_{c2} and λ were calculated within the weak-coupling TB anisotropic BCS model by introducing average parameters. The results of these calculations are also in agreement with the above-presented TB GL theory calculations. The anisotropy parameter γ_λ of London penetration depth was evaluated for two-band superconductors with arbitrary interband and intraband scattering times using the Eilenberger theory in Ref. [88].

As shown by Bulaevskii [89], the upper critical field in the case of SB layered superconductors is defined by the expressions

$$H_{c2}^{\parallel} = \frac{\Phi_0}{2\pi\xi_\perp\xi_\parallel}\,, \qquad H_{c2}^{\perp} = \frac{\Phi_0}{2\pi\xi_\parallel^2}\,.$$

Notice that in this event the anisotropy parameter $\gamma_{H_{c2}}$ proves to be temperature-independent. As stated at the beginning, all the coefficients α and β in the GL model are field-indepen-

dent. Another generalization of the model considered focuses on introducing field-dependent parameters α and β. It is necessary to remark on the very recent paper that took into account the field-dependent TB GL theory without the intergradient interaction term [90].

4. Conclusions

The single-band GL theory gives a well-known linear temperature dependence of the upper, lower, and thermodynamic critical fields: H_{c1}, H_{c2}, and $H_{cm} \propto 1 - T/T_c$. It was noted that single-band calculations were found to be inadequate for describing the temperature dependence of fields, while the two-gap model was found to be satisfactory. We claim that the two-band isotropic GL theory can successfully be applied to determining the temperature dependence of critical fields in bulky nonmagnetic MgB_2, $LuNi_2B_2C$, and YNi_2B_2C borocarbides. The presence of two order parameters and their coupling plays a significant role in determining their temperature dependences. The results of such calculations are in good agreement with experimental data for bulk nonmagnetic borocarbides and magnesium diboride.

We also conclude that the two-band GL theory explains the reduced magnitude of the specific heat jump and the small slope of the thermodynamic magnetic field in MgB_2. It is shown that the relation between the upper critical field and the so-called surface critical field is the same as in the case of single-band superconductors. The temperature dependence of the surface critical field in two-band superconductors must give positive curvature. The quantization of magnetic flux in the case of two-band SCs remains the same as in single-band SCs. However, the periodicity of Little – Parks oscillations of T_c in two-band superconductors is absent. The generalization of the TB GL theory to the case of layered anisotropy was presented. We have calculated the anisotropy parameter of the upper critical field H_{c2} and London penetration depth λ for magnesium diboride single crystals. The temperature-dependent anisotropy of the upper critical field is shown, which, in an agreement with experimental data for MgB_2, reveals the opposite temperature tendency.

Acknowledgments

I am grateful to Abdus Salam ICTP for the hospitality, F Hashimzade for support, and S-L Drechsler for stimulating discussions. I also thank H Yilmaz, M Saglam, A Vercin, B Unal, M Zengin, M Birey, and A Gencer at Ankara University for their hospitality, and N Guclu, A Kilic, and Derya Kanbur for their technical help. This work has been financially supported in part by TUBITAK research grant No. 104T522 (2005) and NATO reintegration grant No. 980766.

References

1. Nagamatsu J et al. *Nature* **410** 63 (2001)
2. Glowacki B A et al. *Supercond. Sci. Technol.* **14** 193 (2001)
3. Gencer A *Supercond. Sci. Technol.* **15** 247 (2002)
4. Bud'ko S L et al. *Phys. Rev. Lett.* **86** 1877 (2001)
5. Kotegawa H et al. *Phys. Rev. Lett.* **87** 127001 (2001)
6. Kortus J et al. *Phys. Rev. Lett.* **86** 4656 (2001)
7. Liu A Y, Mazin I I, Kortus J *Phys. Rev. Lett.* **87** 087005 (2001)
8. Chen X K et al. *Phys. Rev. Lett.* **87** 157002 (2001)
9. Giubileo F et al. *Phys. Rev. Lett.* **87** 177008 (2001)
10. Bouquet F et al. *Phys. Rev. Lett.* **87** 047001 (2001)
11. Nagarajan R et al. *Phys. Rev. Lett.* **72** 274 (1994)
12. Cava R J et al. *Nature* **367** 146 (1994)
13. Drechsler S-L et al. *Physica C* **317 – 318** 117 (1999)
14. Pickett W E, Singh D J *Phys. Rev. Lett.* **72** 3702 (1994)
15. Mattheiss L F *Phys. Rev. B* **49** 13279 (1994)
16. Ravindran P, Johansson B, Eriksson O *Phys. Rev. B* **58** 3381 (1998)
17. Suh B J et al. *Phys. Rev. B* **53** R6022 (1996)
18. Heinecke M, Winzer K *Z. Phys. B* **98** 147 (1995)
19. Freudenberger J et al. *Physica C* **306** 1 (1998)
20. Nohara M et al. *J. Phys. Soc. Jpn.* **66** 1888 (1997)
21. Müller K-H et al. *J. Alloys Comp.* **322** L10 (2001)
22. Bud'ko S L et al. *Phys. Rev. B* **63** 220503 (2001)
23. Shulga S V et al. *Phys. Rev. Lett.* **80** 1730 (1998)
24. Shulga S V et al., cond-mat/0103154
25. Moskalenko V A *Fiz. Met. Metalloved.* **8** 503 (1959) [*Phys. Met. Metallogr.* **8** 25 (1959)]
26. Suhl H, Matthias B T, Walker L R *Phys. Rev. Lett.* **3** 552 (1959)
27. Udomsamuthirun P et al. *Physica C* **425** 149 (2005)
28. Wang Y, Plackowski T, Junod A *Physica C* **355** 179 (2001)
29. Golubov A A et al. *J. Phys.: Condens. Matter* **14** 1353 (2002)
30. Ginzburg V L, Landau L D *Zh. Eksp. Teor. Fiz.* **20** 1064 (1950) [Translated into English: Landau L D *Collected Papers* (Oxford: Pergamon Press, 1965) p. 546]
31. Doh H et al. *Phys. Rev. Lett.* **83** 5350 (1999)
32. Askerzade I N, Gencer A, Güçlü N *Supercond. Sci. Technol.* **15** L13 (2002)
33. Askerzade I N et al. *Supercond. Sci. Technol.* **15** L17 (2002)
34. Moskalenko V A *Zh. Eksp. Teor. Fiz.* **51** 1163 (1966) [*Sov. Phys. JETP* **24** 780 (1967)]
35. Abrikosov A A *Osnovy Teorii Metallov* (Fundamentals of the Theory of Metals) (Moscow: Nauka, 1987) [Translated into English (Amsterdam: North-Holland, 1988)]
36. Saint-James D, De Gennes P G *Phys. Lett.* **7** 306 (1963)
37. Abrikosov A A *Zh. Eksp. Teor. Fiz.* **47** 720 (1964) [*Sov. Phys. JETP* **20** 480 (1965)]
38. Tinkham M *Introduction to Superconductivity* 2nd ed. (New York: McGraw-Hill, 1996)
39. Askerzade I N *Mod. Phys. Lett. B* **18** 1525 (2004)
40. Askerzade I N *Physica C* **397** 99 (2003)
41. Askerzade I N, Gencer A *J. Phys. Soc. Jpn.* **71** 1637 (2002)
42. Askerzade I N *Physica C* **390** 281 (2003)
43. Takahashi K et al. *Phys. Rev. B* **66** 012501 (2002)
44. Zehetmayer M et al. *Phys. Rev. B* **66** 052505 (2002)
45. Lawrence W E, Doniach S, in *Proc. of the 12th Intern. Conf. on Low Temperature Physics, Kyoto, 1970* (Ed. E Kanda) (Tokyo: Kcegaku, 1971) p. 361
46. Bulaevskii L N, in *Problema Vysokotemperaturnoi Sverkhprovodimosti* (High-Temperature Superconductivity) (Eds V L Ginzburg, D A Kirzhnits) (Moscow: Nauka, 1977) [Translated into English (New York: Consultants Bureau, 1982)]
47. Clem J R *Phys. Rev. B* **43** R2991 (1996)
48. Abramowitz M, Stegun I A (Eds) *Handbook on Mathematical Functions, with Formulas, Graphs, and Mathematical Tables* (New York: Dover Publ., 1972) [Translated into Russian (Moscow: Nauka, 1979)]
49. Askerzade I N *Pis'ma Zh. Eksp. Teor. Fiz.* **81** 717 (2005) [*JETP Lett.* **81** 583 (2005)]
50. Udomsamuthirun P et al. *Physica C* **434** 62 (2006)
51. Drechsler S-L, in *High-T_c Superconductors and Related Materials* (NATO Science Ser., Ser. 3, Vol. 86, Eds S-L Drechsler, T Mishonov) (Dordrecht: Kluwer Acad. Publ., 2001) p. 167
52. Uchiyama H et al. *Phys. Rev. Lett.* **88** 157002 (2002)
53. Servedio V D P, Drechsler S-L, Mishonov T *Phys. Rev. B* **66** 140502 (2002)
54. Welp U et al. *Phys. Rev. B* **67** 012505 (2003)
55. Horvat J et al. *Appl. Phys. Lett.* **80** 829 (2002)
56. Zharkov G F *Phys. Rev. B* **63** 214502 (2001)
57. Gorokhov D A *Phys. Rev. Lett.* **94** 077004 (2005)
58. Ghosh K et al. *Phys. Rev. B* **52** 68 (1995)
59. Gurevich A et al. *Supercond. Sci. Technol.* **17** 278 (2004)
60. Patnaik S et al. *Supercond. Sci. Technol.* **14** 315 (2001)
61. Jung M H et al. *Chem. Phys. Lett.* **343** 447 (2001)
62. Ferrando V et al. *Supercond. Sci. Technol.* **16** 241 (2003)
63. Mikheenko P et al. *Mod. Phys. Lett. B* **17** 675 (2003)
64. Landau I L, Ott H R *Physica C* **411** 83 (2004)

65. Zhang Y et al. *Appl. Phys. Lett.* **79** 3995 (2001)
66. Brinkman A et al. *Appl. Phys. Lett.* **79** 2420 (2001)
67. Moskalenko V A, Palistrant M E, Vakalyuk V M *Fiz. Nizk. Temp.* **15** 378 (1989)
68. Mishonov T, Penev E *Int. J. Mod. Phys. B* **16** 3573 (2002)
69. Askerzade I N *Mod. Phys. Lett. B* **17** 11 (2003)
70. Kunchur M N, Lee S-I, Kang W N *Phys. Rev. B* **68** 064516 (2003)
71. Kunchur M N *J. Phys.: Condens. Matter* **16** R1183 (2004)
72. Sologubenko A V et al. *Phys. Rev. B* **65** 180505 (2002)
73. Lyard L et al. *Phys. Rev. B* **66** 180502 (2002)
74. Angst M et al. *Physica C* **385** 143 (2003)
75. Miranović P, Machida K, Kogan V G *J. Phys. Soc. Jpn.* **72** 221 (2003)
76. Kogan V G *Phys. Rev. B* **66** 020509 (2002)
77. Bando H et al. *Physica C* **412** 258 (2004)
78. Angst M et al. *Phys. Rev. Lett.* **88** 167004 (2002)
79. Klemm R A, Luther A, Beasley M R *Phys. Rev. B* **12** 877 (1975)
80. Chandrasekhar B S *Appl. Phys. Lett.* **1** 7 (1962)
81. Clogston A M *Phys. Rev. Lett.* **9** 266 (1962)
82. Drechsler S-L et al. *Physica C* **408–410** 104 (2004)
83. Dao V-H, Zhitomirsky M E *Eur. Phys. J. B* **44** 183 (2005)
84. Zhitomirsky M E, Dao V-H *Phys. Rev. B* **69** 054508 (2004)
85. Koshelev A E, Golubov A A *Phys. Rev. Lett.* **92** 107008 (2004)
86. Lyard L et al. *Phys. Rev. Lett.* **92** 057001 (2004)
87. Cubitt R et al. *Phys. Rev. Lett.* **90** 157002 (2003)
88. Kogan V G, Zhelezina N V *Phys. Rev. B* **69** 132506 (2004)
89. Bulaevskii L N *Zh. Eksp. Teor. Fiz.* **64** 2241 (1973) [*Sov. Phys. JETP* **37** 1133 (1973)]
90. Eisterer M et al. *Phys. Rev. B* **72** 134525 (2005)